

Electrophysical Properties of Composites Based on Polyethylene Modified with Multi-Walled Carbon Nanotubes with High Content of Fe–Co-Catalyst

S. I. Moseenkov^{a,*}, V. L. Kuznetsov^{a,b}, A. V. Zavorin^{a,b}, G. V. Golubtsov^{a,b}, E. Yu. Korovin^c,
V. I. Suslyayev^c, A. V. Ishchenko^a, A. N. Serkova^a, D. I. Sergeenko^c, and D. A. Velikanov^d

^a Boreskov Institute of Catalysis of the Siberian Branch of the Russian Academy of Sciences, Novosibirsk, 630090 Russia

^b Novosibirsk National Research State University, Novosibirsk, 630090 Russia

^c National Research Tomsk State University, Tomsk, 634050 Russia

^d Kirensky Institute of Physics of the Siberian Branch of the Russian Academy of Sciences, Krasnoyarsk, 660036 Russia

*e-mail: moseenkov@catalysis.ru

Received April 11, 2019; revised November 22, 2019; accepted December 14, 2019

Abstract—The effect of the residual catalyst for the synthesis of multi-walled carbon nanotubes (MWCNTs) on the electrophysical properties of MWCNT–polyethylene composites produced by melt mechanical mixing was studied. The residual catalyst content was varied by changing the MWCNTs synthesis time. The nanotubes used in the work were characterized using transmission and scanning electron microscopy, atomic emission analysis, X-ray phase analysis, and magnetic permeability measurements. The structure of the synthesized composites was studied using optical and scanning electron microscopy. The dependences of the specific magnetization on the applied magnetic field, bulk electrical conductivity on the volumetric content of the filler in the composite, and the frequency dependences of the reflection, transmission, and absorption of electromagnetic radiation in the range 0.01–18 GHz were obtained. It was established that the obtained composites are characterized by a uniform distribution of nanotubes in the polymer matrix, and the dependence of the bulk electrical conductivity on the content of MWCNTs in the composite has a percolation character. Variation in the synthesis time of nanotubes allows producing MWCNTs with a high content of ferromagnetic particles, which are an alloy close in stoichiometry to the composition of the active component of the catalyst. It was shown that the use of composites modified with MWCNTs with a high content of residual catalyst is more effective for absorbing electromagnetic radiation due to an increase in their magnetic losses.

Keywords: multi-walled carbon nanotubes, ferromagnetic catalyst particles, polymer composites, mechanical mixing in the melt, gigahertz range, electromagnetic absorption

DOI: 10.1134/S107042722004014X

Owing to the unique physicochemical properties [1–3], multilayered carbon nanotubes (MWCNTs) are of interest to researchers around the world and are one of the main materials of developing nanotechnologies. Due to the high electrical conductivity and high aspect ratio, the introduction of small amounts of MWCNTs into polymer or ceramic matrices makes it possible to increase the electrical conductivity of the resulting composites by 5–10 orders of magnitude [4]. At the same time, varying the characteristics of MWCNTs (external diameter, length, functional composition of

the surface), their content in the composite and the method for producing the composite allows controlling the distribution of nanotubes in the resulting material, which opens up wide possibilities for using the resulting composites as functional materials [5–7], for example, to increase the electromagnetic compatibility of devices.

The rapid growth in the number of devices using wireless data transmission leads to pollution by electromagnetic radiation of the environment and has an impact on human health and the normal functioning of electronics. This fact increases the relevance of the

development of materials to increase electromagnetic compatibility, which are usually utilized materials with high dielectric and magnetic losses. Dielectric losses are defined as $D_e = \epsilon''/\epsilon'$ (ϵ' and ϵ'' are the real and imaginary parts of the dielectric constant), depend on the conductivity of the material and characterize the dissipation of energy created by an external electric field. Magnetic losses $D_m = \mu''/\mu'$ (μ' and μ'' are the real and imaginary parts of the magnetic susceptibility) correspond to the energy loss inside the magnetic material due to the phase delay between the applied and induced magnetic fields and characterize the dissipation of the energy created by the external magnetic field. To minimize the reflection of electromagnetic radiation from the absorber, it is also necessary to match the wave resistance of the absorbing medium and free space [8]. Reflection losses [Eq. (1)] and wave resistance of the material [Eq. (2)] are defined as [9]

$$RL = 20 \log \left| \frac{Z - Z_0}{Z + Z_0} \right|, \quad (1)$$

$$Z = Z_0 \sqrt{\frac{\mu}{\epsilon}} \tanh \left(i 2\pi f d / c \sqrt{\frac{\mu}{\epsilon}} \right), \quad (2)$$

where Z is wave impedance of material, Z_0 is free space wave impedance (377 Ω), $\epsilon = \epsilon' - i\epsilon''$ and $\mu = \mu' - i\mu''$ is complex dielectric and magnetic permeabilities, respectively, f is the frequency, c is the speed of light, d is the layer thickness, $i^2 = -1$.

In contrast to materials with dielectric losses, materials with magnetic losses (or with dielectric and magnetic losses simultaneously) for the problems of increasing electromagnetic compatibility have been actively studied only in recent years [10–15]. Magnetic losses in composites with dispersed magnetic particles are determined by relaxation mechanisms of their magnetic moment [16, 17]. Ferromagnetic metals (Fe, Ni, Co) and their alloys have high values of magnetic saturation, but due to the high conductivity, eddy current losses lead to a decrease in magnetic permeability [18], therefore, a decrease in the size of magnetic particles below critical [nineteen] is required for the effective absorption of electromagnetic radiation. As the nanoparticle size decreases, a transition from the ferromagnetic state to the superparamagnetic state occurs, which results to an additional increase in the relaxation frequency [20, 21], and the presence of physical contact between magnetic

nanoparticles prevents spin fluctuations [22], which leads to a decrease in the particle relaxation frequency. Thus, to expand the working frequency range of composites with magnetic losses and the effective use of magnetic particles, it is necessary to create a material with a uniform distribution of magnetic particles of a minimum size.

It is known that for the synthesis of MWCNTs, some of the most effective catalysts are those based on Fe and Co [23]. Active catalytic particles of the Fe–Co alloy are formed at the activation stage and are comparable in size to the outer diameter of the nanotubes growing on them. Controlling the MWCNTs synthesis time makes it possible to produce nanotubes with an increased content of dispersed magnetically active particles of the Fe–Co alloy formed at the stage of activation of the catalyst, and carbonization or encapsulation of alloy particles in the channels of MWCNTs occurring during deactivation of the catalyst prevents the particles from oxidizing when the sample is carried out to air.

The purpose of the work is to synthesize composites based on a polyethylene matrix modified with MWCNTs with a high content of magnetically active particles of the Fe–Co alloy having both dielectric and magnetic losses, and to perform a comparative study of the effect of magnetically active particles on the interaction of such composites with electromagnetic radiation in the gigahertz frequency range.

EXPERIMENTAL

Multi-walled carbon nanotubes were obtained using chemical vapor deposition by decomposition of a mixture of ethylene with argon (1 : 1) at 680°C on a catalyst with an active component of the composition Fe_2Co [24]. The content of ferromagnetic catalyst particles in MWCNTs was controlled by changing the nanotube growth time. We used two types of MWCNTs with a total Fe and Co content (according to atomic emission analysis) of 1.1 and 25.2 wt % for NT and NT-k samples, for which the synthesis duration was 15 and 3 min, respectively.

To synthesize composites with polyethylene (Daelim LH3750m), weighed samples of MWCNTs and polyethylene were mixed in a knife mill for 3 min until a uniform mixture was obtained. The resulting mixture was processed on a Dynisco LME mixing extruder. A feature of this mixing extruder is the ability to control the gap between the rotating shaft and the fixed head

through which the composite melt passes. The size of the gap determines the maximum size of the passing particles and the intensity of shear deformation in the melt, contributing to the destruction of the aggregates of nanotubes. The treatment was carried out at a screw temperature of 135°C and a head temperature of 145°C in two stages. First, the powder mixture was fused at a gap between the screw and the head of 500 µm, then the MWCNTs were dispersed in the polymer by seven successive treatments with a distance between the screw and the head of 100 µm. Films of composites with a thickness of 500 ± 10 µm were obtained by hot pressing for 5 min at 140°C and a pressure of 2 MPa. Using this technique, C-NT composites were produced with a content of nanotubes NT 0.83, 1.3, 2.1, 3.2, 4.3, and 5.5 vol % nanotubes and C-NT-k composites with a content of nanotubes NT-k 0.84, 1.3, 2.1, 3.3, 4.4 and 5.6 vol %.

The initial MWCNTs were characterized using transmission electron microscopy (TEM, JEM-2010, Jeol), scanning electron microscopy (SEM, JSM6460LV, Jeol), X-ray phase analysis (XRD, ARL X'TRA, Thermo Scientific). The magnetic permeability of MWCNT powders was determined by changing the impedance modulus and phase shift of the complex resistance of the coil into which the test sample was introduced (MNIPI E7-30). The obtained values were recalculated taking into account the degree of coil filling and bulk density of the samples (0.13 and 0.085 g cm⁻³ for NT and NT-k, respectively).

The structure of the synthesized composites was studied using optical microscopy (BioMed 5) and SEM. A sample for optical microscopy was obtained by melting the composite between slides at 150°C and a pressure of 1 MPa. SEM studies were performed on fractures of composites films obtained by their destruction under a layer of liquid nitrogen. To prevent recharging and destruction of the sample, a thin (~10 nm) layer of gold was deposited on the test surface. The specific magnetization of the composites was measured as a function of the magnetic field strength using a 7410 VSM vibration magnetometer (Lake Shore) in fields up to 20 kOe. The bulk conductivity of the composites was determined from measurements of the current – voltage characteristic, which were performed using a Keithley 6487 source meter and a Keithley 8009 measuring chamber. The specific conductivity was

calculated using the data of the third measurement of the current–voltage characteristic in the region of the linear dependence of the current on voltage for all composites at electric field strength of 3 V mm⁻¹. The frequency dependences of reflection, transmission, and absorption in the range of 0.01–18 GHz were determined in an N-type coaxial cell using an N5247A network analyzer (Agilent Technologies) [25].

RESULTS AND DISCUSSION

The structure and properties of the initial MWCNTs. Using the TEM and SEM methods, the structure of the initial MWCNTs NT and NT-k was studied (Fig. 1). It was found by TEM that particles of the Fe–Co alloy are present in the structure of MWCNT samples mainly in the form of two types of particles: nanotubes encapsulated in the channels with a size of 4–8 nm (Fig. 1a) and in the form of carbonized particles with a size of 10–15 nm (Figs. 1b, 1c). The presence of encapsulated particles of the Fe–Co alloy in the MWCNT channels is associated with the catalyst deactivation process, when the working particles of the active component are partially drawn into the channel of the formed nanotube, and that of the carbonized particles of the Fe and Co alloy, with sintering the dispersed active component during catalyst activation and their subsequent carbonization [23]. According to TEM, the size of carbonized particles does not depend on the MWCNTs synthesis time.

Using the SEM method (Figs. 1d–1g), it was found that the residual catalyst is flattened particles of finely dispersed spinels based on Fe, Co, and Al [26]. Growing nanotubes form dense strands on the surface of the catalyst. In NT-k samples, the length of MWCNT strands was 5–10 µm, and in NT samples it was 15–25 µm (Figs. 1f, 1g), which is associated with different nanotube synthesis times. It has been established that MWCNT strands consist of contacting single intertwined nanotubes. In addition, the NT-k sample bulk contains a significant amount of catalyst carrier particles (Fig. 1d, insert) with an average size of 50–70 µm, which can structure MWCNTs and facilitate their dispersion in the polymer matrix.

The analysis of X-ray diffraction patterns of NT and NT-k samples showed the presence of reflexes $2\theta = 25^\circ$ (002) and $2\theta = 43^\circ$ (111), characteristic of nanotubes (Fig. 2). For the NT-k sample, the intensity of these peaks is lower than for the NT sample. In the

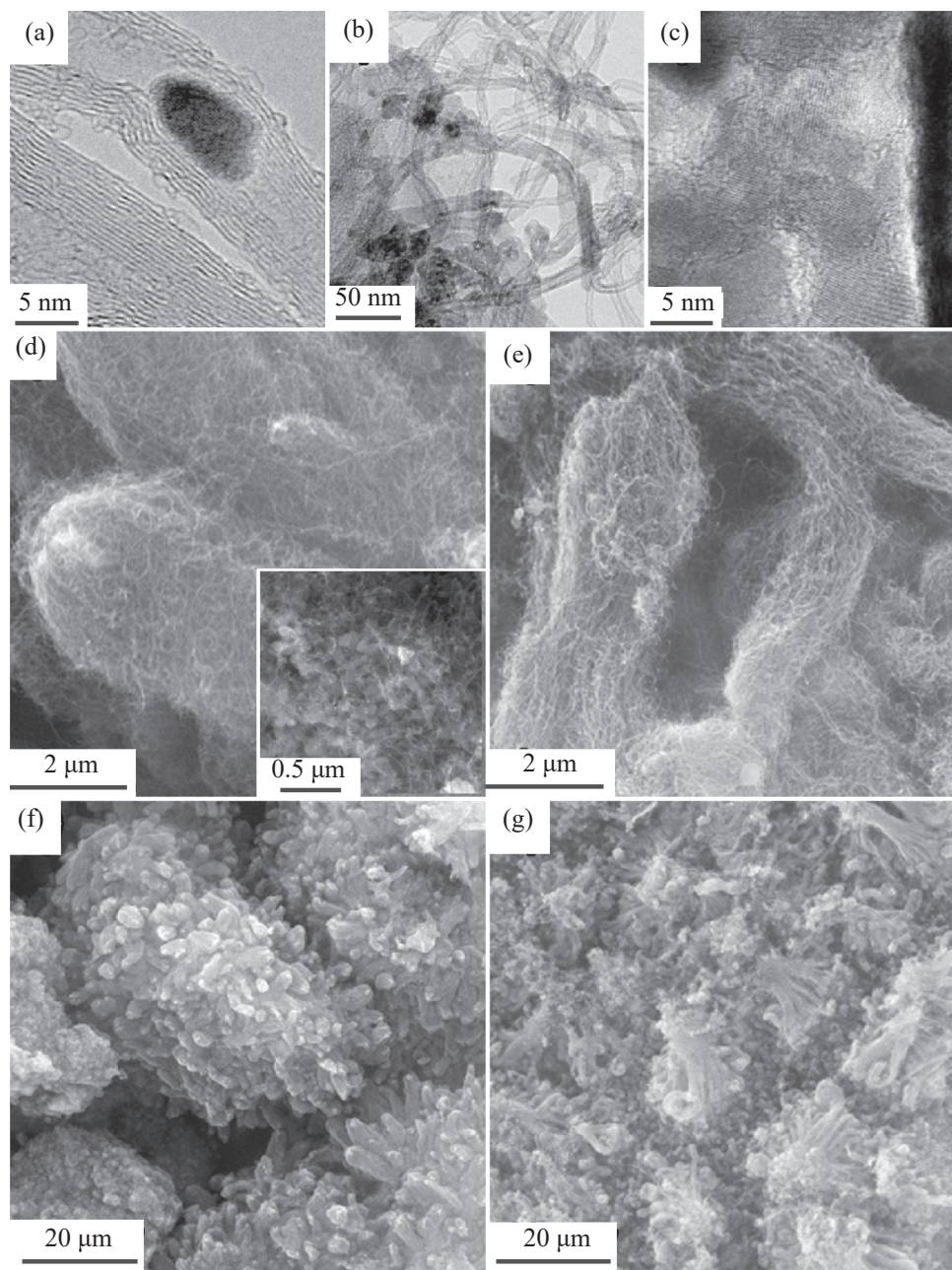


Fig. 1. TEM and REM images of multi-walled carbon nanotubes samples of different synthesis times. (a–c) TEM images of the NT-k sample; (d, f) SEM images of the NT-k sample; (e, g) SEM images of the NT sample.

X-ray diffraction pattern of NT-k sample there are peaks characteristic of spinel phases based on Al_2O_3 in the composition of the catalyst support and active Fe–Co particles [27]. Due to the absence of peaks characteristic of metallic Co on the X-ray diffraction pattern, it can be assumed that Fe and Co metals form an alloy of Fe_2Co composition corresponding to the composition of the active component of the catalyst.

The frequency dependences of the magnetic permeability of MWCNTs NT and NT-k samples were obtained (Fig. 3). It was established that μ' , μ'' and the tangent of the magnetic loss angle of the samples have a similar frequency dependence in the range of 10 kHz–3 MHz, and differences in their absolute value are caused by different contents of magnetic particles. It was determined that the magnetic permeability depends

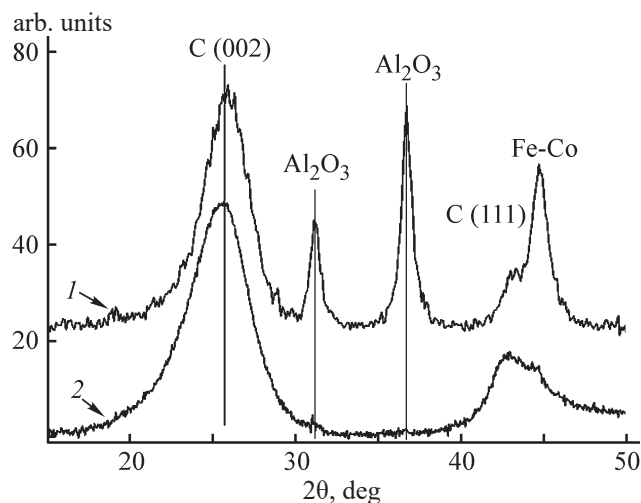


Fig. 2. X-ray diffraction patterns of the initial multi-walled carbon nanotubes samples: (1) NT-k and (2) NT.

nonlinearly on the metal content in the sample, since the total Fe and Co content in the NT-k sample is 22.8 times greater than in the NT sample (according to atomic emission analysis), while the magnetic permeability of the NT-k sample is 3 times the size of NT. This difference is apparently caused by the partial oxidation of metal particles in the NT-k sample with atmospheric oxygen.

Thus, the results of a study of the initial MWCNTs NT and NT-k using TEM, SEM, and XRD methods and

by determining the frequency dependence of magnetic permeability showed that it is possible to effectively control the content of Fe_2Co particles in the resulting nanotubes and the magnetic permeability of MWCNTs by changing the their synthesis time.

Study of the structure and properties of composites. The structure of the composites was investigated using optical microscopy and SEM (Fig. 4).

Using the method of optical microscopy, it was found that the optical density of the matrix of composites varies slightly over the entire image field. The structure of the composites contains a small amount of dense black inclusions of 5–10 μm in size (Figs. 4a, 4b), which are aggregates of nanotubes. On the SEM images of the composites, no large inclusions, aggregates or strands of MWCNTs are observed (Figs. 4e, 4f). High-resolution SEM images showed that single nanotubes and the most durable primary MWCNT aggregates 200–400 nm in size are observed on the surface (Figs. 4c, 4d). Thus, the study of the structure of composites by optical microscopy and SEM allows to conclude that due to intense mechanical stress during the preparation of composites, the majority of primary nanotube aggregates are destroyed, and the resulting composites have a high uniformity of the distribution of nanotubes in the polymer matrix.

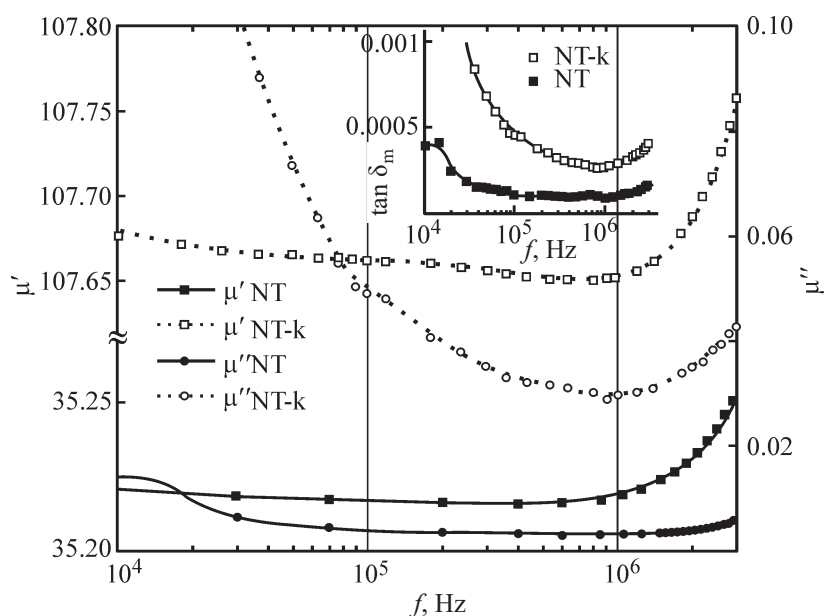


Fig. 3. Frequency dependence of the magnetic permeability of NT and NT-k multi-walled carbon nanotube samples, adjusted for their bulk density. The inset shows the frequency dependence of the magnetic loss tangent for NT and NT-k samples.

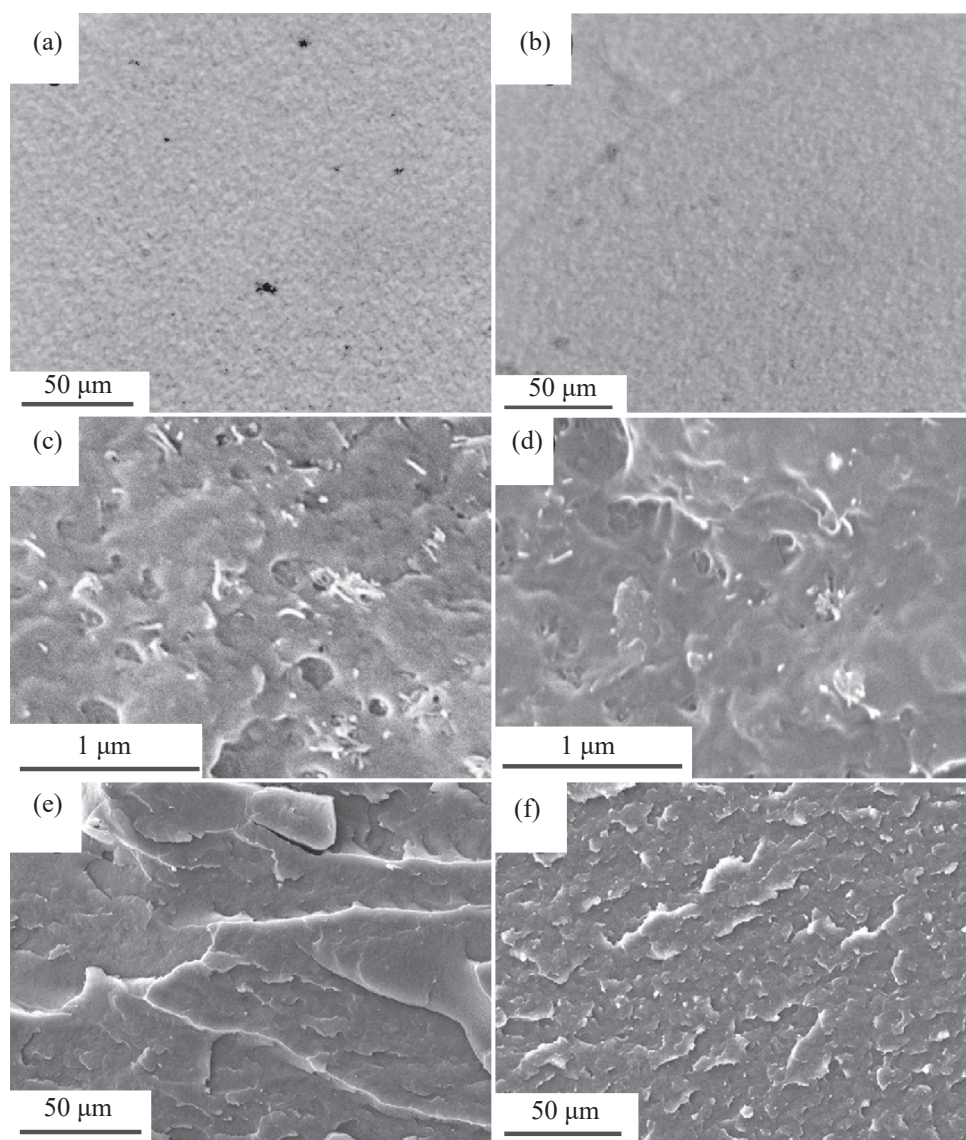


Fig. 4. Typical images of composites using samples with the same nanotube content: (a) 2.1 vol % C-NT and (b) 2.1 vol % C-NT-k, obtained using (a, b) optical microscopy and (c–f) scanning electron microscopy.

Using a vibration magnetometer, data were obtained on the dependence of the specific magnetization on the applied magnetic field for samples of composites 5.5 vol % C-NT and 5.6 vol % C-NT-k (Fig. 5).

The non-linear character of the magnetization curves and the presence of hysteresis indicate the presence of ferromagnetic particles in the composites. It was found that for a 5.5 vol % C-NT composite, the coercive force and magnetic saturation are $75 \text{ G cm}^3 \text{ g}^{-1}$ and 1600 Oe, and for a 5.6 vol % C-NT-k composite, $105 \text{ G cm}^3 \text{ g}^{-1}$ and 2300 Oe, respectively. The large value of magnetic saturation for the 5.6 vol % C-NT-k sample indicates an increase in the fraction of magnetic particles in it com-

pared to the 5.5 vol % C-NT sample. An increase in the coercive force with an increase in the content of metal particles occurred for composites is consistent with an increase in the size of metal particles from 4–8 for MWCNT NT to 10–15 nm for MWCNT NT-k, determined by the TEM method. Due to the small size, magnetic particles in all composites are single-domain [28, 29]. The results are also consistent with the data on the mechanism of catalyst deactivation for the MWCNTs synthesis, when fragments of catalytic particles in the internal channel of nanotubes in the form of metal particles 4–8 nm in size (corresponding to the diameter of the internal channel in nanotubes) are periodically encap-

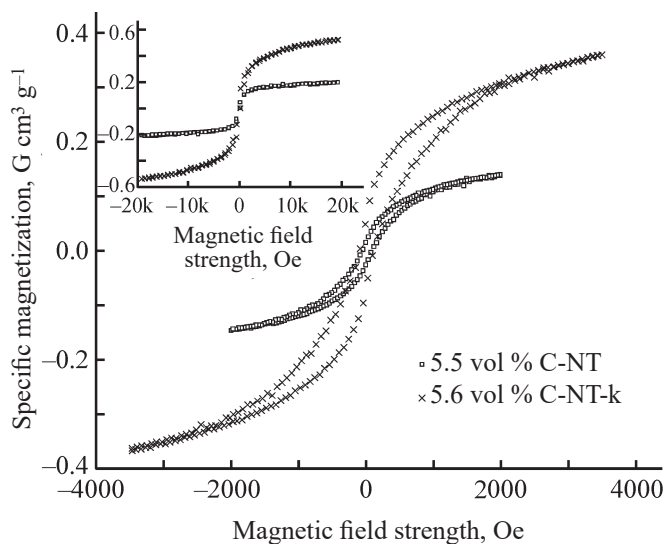


Fig. 5. Specific magnetization vs. the magnetic field strength in the range of ± 3500 Oe for samples of composites 5.5 vol % C-NT and 5.6 vol % C-NT-k. On the inset the specific magnetization of these samples vs. the magnetic field strength in the range of ± 20 kOe.

sulated during nanotube growth. This process continues until the size of the catalytic particle becomes equal to or smaller than the diameter of the growing nanotube and leads to the final dispersion of the active component.

It was established that the dependence of the bulk electrical conductivity of the composites on the volumetric content of MWCNTs at constant current (Fig. 6) has a percolation character. C-NT-k composites

are characterized by a higher conductivity value in comparison with C-NT composites at a close MWCNT content.

An approximation of the obtained concentration dependences of the bulk electrical conductivity of composites with the theoretical function $\sigma \sim (p - p_c)^t$ [30] (Fig. 6, inset) made it possible to establish the values of the critical concentration of MWCNTs (p_c) and the critical conductivity index (t) depending on the MWCNTs used: for C-NT composites $p_c = 0.77$ and $t = 3.93$; for C-NT-k composites $p_c = 1.04$ and $t = 2.85$. Thus, due to shorter synthesis time and, correspondingly, shorter nanotube lengths, C-NT-k composites have a higher percolation threshold than C-NT composites. Moreover, the high bulk electrical conductivity of the C-NT-k composites as compared to the C-NT composites at a close content of nanotubes indicates a greater number of contacts between individual nanotubes in the composite. The reason for this fact may be the residual catalyst, which contributes to the destruction of MWCNT aggregates during the preparation of C-NT-k composites.

A study of the frequency dependence of the reflection, transmission, and absorption of electromagnetic radiation with composites in the range 0.01–18 GHz (Fig. 7a) showed that all samples are characterized by an increase in absorption and reflection and a decrease in transmittance with increasing frequency. For C-NT-k composites in the frequency range of 14–18 GHz, a change in the nature of the frequency dependence of

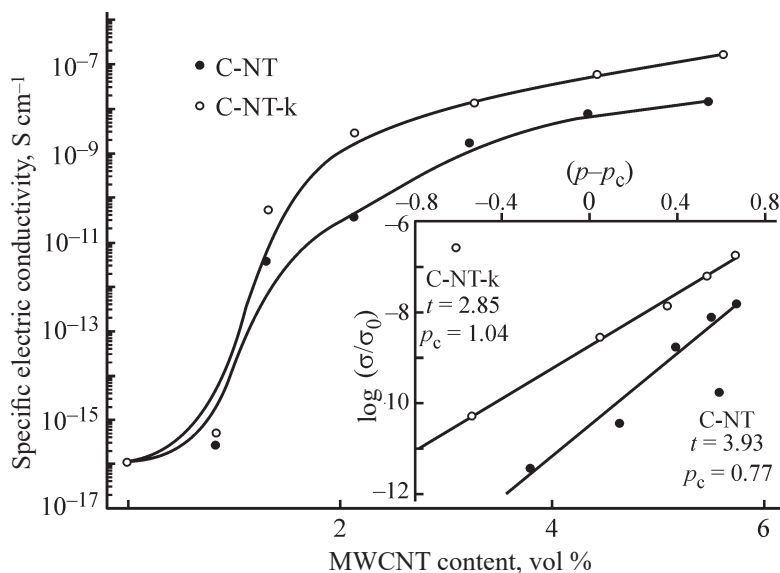


Fig. 6. Bulk DC conductivity vs. volumetric concentration of multi-walled carbon nanotubes in C-NT and C-NT-k composites. The inset shows the approximation of bulk electrical conductivity data by the function $\sigma \sim (p - p_c)^t$.

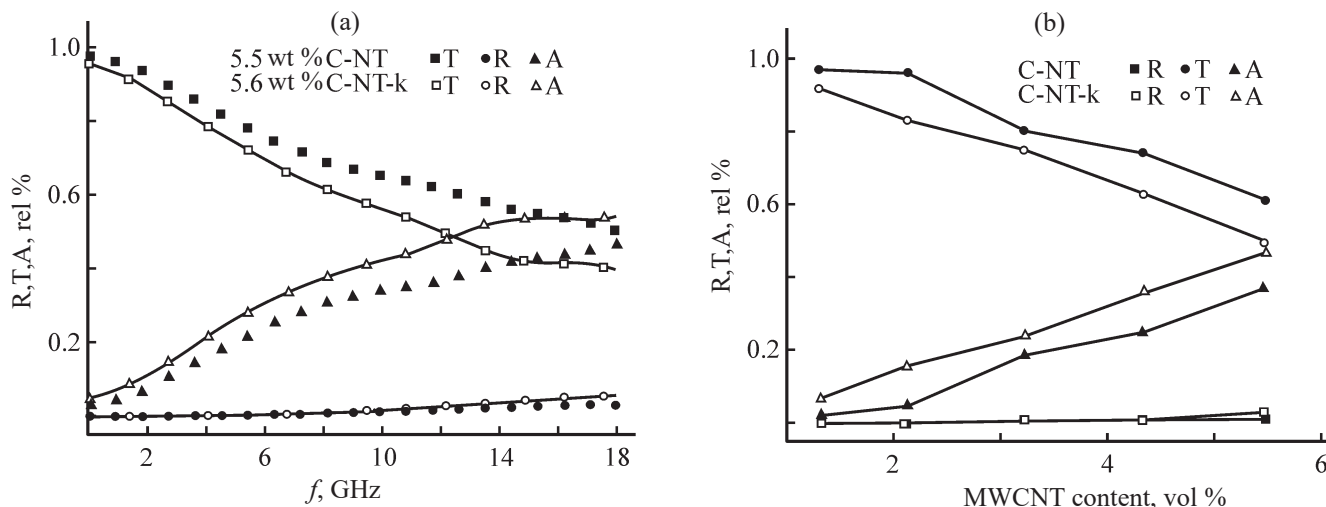


Fig. 7. (a) Typical frequency dependences of transmittance (T), reflection (R) and absorption (A) on the example of composites 5.5 vol % C-NT and 5.6 vol % C-NT-k and (b) the dependence of transmittance, reflection and absorption on the volumetric content of multi-walled carbon nanotubes in composites C-NT and C-NT-k at a fixed frequency of 12 GHz.

absorption and transmission occurs in comparison with C-NT composites.

It can be seen that, over the entire range of MWCNT concentrations, C-NT-k composites exhibit greater absorption and lower transmission of electromagnetic radiation (Fig. 7b). This effect can only be explained by the presence of magnetic losses in the composites. It should be noted that when in 5.5 vol % C-NT and 5.6 vol % C-NT-k composites there are MWCNTs, the mass content of metals in them is ~ 0.1 and 2.5 wt %, respectively. This suggests that an increase in the metal content in the composite to 10–15 wt % due to a further decrease in the MWCNTs synthesis time or an increase in the MWCNTs content in the composite can significantly enhance the effect of absorption of electromagnetic radiation in the gigahertz frequency range.

CONCLUSIONS

It was established that due to a change in the synthesis time of multi-walled carbon nanotubes, it is possible to synthesize samples with a high content of magnetically active metal particles, which are an alloy close in stoichiometry to the composition of the active component of the catalyst. The particles obtained in this way are ferromagnetic. An increase in the synthesis time of multi-walled carbon nanotubes leads to a decrease in the average size of magnetic particles due to their dispersion in the channels of nanotubes.

Reducing the synthesis time of multi-walled carbon nanotubes leads to a decrease in their length and an increase in the content of residual catalyst. The use of such nanotubes for producing composites leads to a slight increase in the percolation threshold and, at the same time, to an increase in the conductivity of the composite above the percolation threshold. An increase in the content of ferromagnetic metal particles in the composite modified with MWCNTs increases the absorption of electromagnetic radiation due to an increase in magnetic losses.

FUNDING

This work was financially supported by the Russian Science Foundation, project no. 17-73-20293.

CONFLICT OF INTEREST

The authors declare that they have no conflict of interest.

REFERENCES

- De Volder, M.F.L., Tawfick, S.H., Baughman, R.H., and Hart, A.J., *Science*, 2013, vol. 339, no. 6119, pp. 535–539. <https://doi.org/10.1126/science.1222453>
- Popov, V., *Mater. Sci. Eng.: R: Reports*, 2004, vol. 43, no. 3, pp. 61–102. <https://doi.org/10.1016/j.mser.2003.10.001>
- Feller, J.-F., Castro, M., and Kumar, B., *Polymer–Carbon Nanotube Composites*, Elsevier, 2011.

4. Bauhofer, W. and Kovacs, J.Z., *Composites Sci. Technol.*, 2009, vol. 69, no. 10, pp. 1486–1498.
<https://doi.org/10.1016/j.compscitech.2008.06.018>
5. Spitalsky, Z., Tasis, D., Papagelis, K., and Galiotis, C., *Progress Polym. Sci.*, vol. 35, no. 3, pp. 357–401.
<https://doi.org/10.1016/j.progpolymsci.2009.09.003>
6. Gong, S., Zhu, Z.H., and Meguid, S.A., *Polymer*, 2015, vol. 56, pp. 498–506.
<https://doi.org/10.1016/j.polymer.2014.11.038>
7. González, M., Pozuelo, J., and Baselga, J., *Chem. Record.*, 2018, vol. 18, nos. 7–8, pp. 1000–1009.
<https://doi.org/10.1002/tcr.201700066>
8. Li, J., Lu, W., Suhr, J., Chen, H., Xiao, J.Q., and Chou, T.-W., *Sci. Reports*, 2017, vol. 7, no. 2349, p. 110.
<https://doi.org/10.1038/s41598-017-02639-7>
9. Wang, G., Gao, Z., Wan, G., Lin, S., Yang, P., and Qin, Y., *Nano Research*, 2014, vol. 7, no. 5, pp. 704–716.
<https://doi.org/10.1007/s12274-014-0432-0>
10. Cheng, H., Wei, S., Ji, Y., Zhai, J., Zhang, X., Chen, J., and Shen, C., *Composites. Part A: Appl. Sci. Manufacturing*, 2019, vol. 121, pp. 139–148.
<https://doi.org/10.1016/j.compositesa.2019.03.019>
11. Liu, Y., Lu, M., Wu, K., Yao, S., Du, X., Chen, G., Zhang, Q., Liang, L., and Lu, M., *Composites Sci. Technol.*, 2019, vol. 174, pp. 1–10.
<https://doi.org/10.1016/j.compscitech.2019.02.005>
12. Lee, S.-H., Kang, D., and Oh, I.-K., *Carbon*, 2017, vol. 111, pp. 248–257.
<https://doi.org/10.1016/j.carbon.2016.10.003>
13. Sankaran, S., Deshmukh, K., Ahamed, M.B., and Khadheer Pasha, S.K., *Appl. Sci. Manufacturing*, 2018, vol. 114, pp. 49–71.
<https://doi.org/10.1016/j.compositesa.2018.08.006>
14. Abbasi, H., Antunes, M., and Velasco, J.I., *Progress Mater. Sci.*, 2019, vol. 103, pp. 319–373.
<https://doi.org/10.1016/j.pmatsci.2019.02.003>
15. Wang, C., Murugadoss, V., Kong, J., He, Z., Mai, X., Shao, Q., Chen, Y., Guo, L., Liu, C., Angaiah, S., and Guo, Z., *Carbon*, 2018, vol. 140, pp. 696–733.
<https://doi.org/10.1016/j.carbon.2018.09.006>
16. Kodama, R.H., *J. Magnetism Magnetic Mater.*, 1999, vol. 200, no. 1, pp. 359–372.
[https://doi.org/10.1016/S0304-8853\(99\)00347-9](https://doi.org/10.1016/S0304-8853(99)00347-9)
17. Dosoudil, R., Usakova, M., Franek, J., Slama, J., and Gruskova, A., *IEEE Transactions on Magnetism*, 2010, vol. 46, no. 2, pp. 436–439.
<https://doi.org/10.1109/TMAG.2009.2033347>
18. Liu, W., Zhong, W., Jiang, H.Y., Tang, N.J., Wu, X.L., and Du, W.Y., *Eur. Phys. J. B—Condensed Matter and Complex Systems*, 2005, vol. 46, no. 4, pp. 471–474.
<https://doi.org/10.1140/epjb/e2005-00276-2>
19. Zhang, X.F., Guan, P.F., and Dong, X.L., *Appl. Phys. Lett.*, 2010, vol. 97, no. 033107, p. 13.
<https://doi.org/10.1063/1.3464975>
20. Liu, X.G., Li, B., Geng, D.Y., Cui, W.B., Yang, F., Xie, Z.G., Kang, D.J., and Zhang, Z.D., *Carbon*, 2009, vol. 47, no. 2, pp. 470–474.
<https://doi.org/10.1016/j.carbon.2008.10.028>
21. Song, N.-N., Yang, H.-T., Liu, H.-L., Ren, X., Ding, H.-F., Zhang, X.-Q., and Cheng, Z.-H., *Sci. Reports*, 2013, vol. 3, no. 3161, p. 15.
<https://doi.org/10.1038/srep03161>
22. Song, N.-N., Ke, Y.-J., Yang, H.-T., Zhang, H., Zhang, X.-Q., Shen, B.-G., and Cheng, Z.-H., *Sci. Reports*, 2013, vol. 3, no. 2291, p. 15.
<https://doi.org/10.1038/srep02291>
23. Usoltseva, A., Kuznetsov, V., Rudina, N., Moroz, E., Haluska, M., and Roth, S., *Physica Status Solidi B*, 2007, vol. 244, no. 11, pp. 3920–3924.
<https://doi.org/10.1002/pssb.200776143>
24. Andreev, A.S., Krasnikov, D.V., Zaikovskii, V.I., Cherepanova, S.V., Kazakova, M.A., Lapina, O.B., Kuznetsov, V.L., and d’Espinose de Lacaillerie, J., *J. Catal.*, 2018, vol. 358, pp. 62–70.
<https://doi.org/10.1016/j.jcat.2017.11.025>
25. Suslyayev, V.I., Kuznetsov, V.L., Zhuravlev, V.A., Mazov, I.N., Korovin, E.Yu., Moseenkov, S.I., and Dorozhkin, K.V., *Russ. Phys. J.*, 2013, vol. 55, no. 8, pp. 970–976.
<https://doi.org/10.1007/s11182-013-9909-7>
26. RF Patent 2373995 (Publ. 2009).
27. Kuznetsov, V.L., Krasnikov, D.V., Schmakov, A.N., and Elumeeva, K.V., *Physica Status Solidi B*, 2012, vol. 249, no. 12, pp. 2390–2394.
<https://doi.org/10.1002/pssb.201200120>
28. Li, Q., Kartikowati, C.W., Horie, S., Ogi, T., Iwaki, T., and Okuyama, K., *Sci. Reports*, 2017, vol. 7, no. 9894, p. 17.
<https://doi.org/10.1038/s41598-017-09897-5>
29. Nascimento, V.P., Passamani, E.C., Takeuchi, A.Y., Larica, C., and Nunes, E., *J. Phys.: Condensed Matter.*, 2001, vol. 13, no. 4, pp. 665–682.
<https://doi.org/10.1088/0953-8984/13/4/313>
30. Eletskii, A.V., Knizhnik, A.A., Potapkin, B.V., and Kenny, J.M., *Physics-Uspekhi*, 2015, vol. 58, no. 3, pp. 209–251.
<https://doi.org/10.3367/UFNe.0185.201503a.0225>